

基于吡嗪连接的石墨烯电极单分子场效应晶体管

孙汉涛^{1,2}, 廖建辉^{1,*}, 侯士敏^{1,2,*}

¹ 北京大学电子学系, 纳米器件物理与化学教育部重点实验室, 北京 100871

² 北京大学纳米科学与技术研究中心, 北京 100871

Single-Molecule Field-Effect Transistors with Graphene Electrodes and Covalent Pyrazine Linkers

Hantao Sun^{1,2}, Jianhui Liao^{1,*}, Shimin Hou^{1,2,*}

¹ Key Laboratory for the Physics and Chemistry of Nanodevices, Department of Electronics, Peking University, Beijing 100871, P. R. China.

² Centre for Nanoscale Science and Technology, Peking University, Beijing 100871, P. R. China.

*Corresponding authors. Emails: smhou@pku.edu.cn (S.H.); jianhui.liao@pku.edu.cn (J.L.).

Tel.: +86-10-62768078 (S.H.); +86-10-62755807 (J.L.).

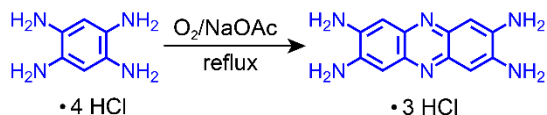
1 Synthetic Method

2 Fabrication Processes of Graphene Nano-gaps

3 Electrical characterization of DPP single-molecule FETs

1 Synthetic Method

The target phenazine derivative was synthesized in a one-step reaction starting with 1,2,4,5-tetraamino-benzene as shown in Scheme S1. Heating an aqueous solution of 1,2,4,5-tetraamino-benzene·4HCl in the presence of NaOAc (sodium acetate) and under a stream of compressed air gave deep purple-colored phenazine-2,3,7,8-tetraamine.



Scheme S1 A synthetic route to the target *ortho*-phenylenediamine terminated phenazine derivative.

2 Fabrication Processes of Graphene Nano-gaps

The graphene structures were fabricated following a previously described procedure, as shown in Fig. S1. Photolithography and electron beam evaporation (5 nm Ti/40 nm Au) were used to define a grid of alignment marks with 500 μm pitches on the silicon wafer coated with 300 nm silicon dioxide. CVD-grown single-layer graphene (SLG) was separated from the copper substrate using the electrolytic bubbling method and transferred to the silicon substrate with the alignment grid. Electron beam lithography (Raith 150 Two) was employed to pattern contact electrodes with channel lengths of 1 μm . Subsequently, metallic source/drain contact electrodes (5 nm Ti/45 nm Au) were deposited using the electron-beam evaporation. Electron beam lithography was used again to pattern windows in PMMA (A4 950k). The SLG between Ti/Au electrodes was etched into a notched ribbon with two extra-narrow (80 nm) grooves using oxygen plasma etching. Finally, Electron beam lithography and metal deposition (5 nm Ti/60 nm Au) were used to define the pad electrodes for measurement. Characterization of the graphene structures before the electro-burning process was shown in Fig. S2. These graphene structures are nearly intrinsic as the Dirac point appears near the zero gate voltage.

We fabricated nano-gaps in the graphene structures using the feedback-controlled electro-burning process performed at room temperature in air. Fig. S3a shows a set of current-voltage curves recorded during the feedback-controlled electro-burning process. One nano-gap was gradually generated in the graphene structure with a fixed target resistance (500 M Ω –1 G Ω). Typical current–voltage characteristics of a graphene nano-gap is shown in Fig. S3b, the current is in the picoampere range when the voltage is varied from -0.5 V to 0.5 V.

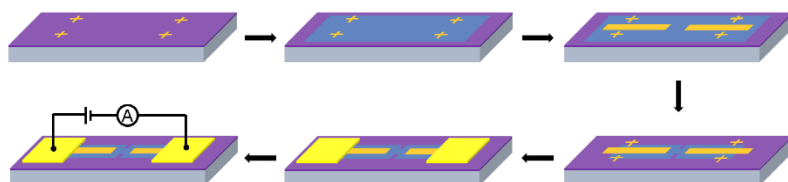


Fig. S1 Schematic of the fabrication procedure to form a graphene structure.

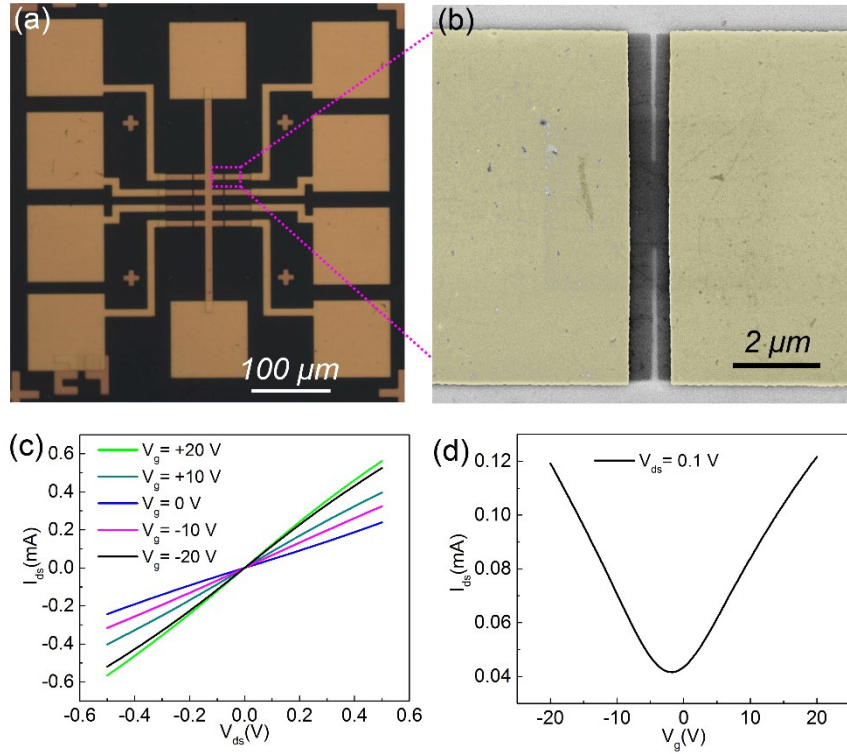


Fig. S2 Characterization of graphene structures before the electroburning process.

(a) Optical microscopy image of graphene devices. (b) SEM image of a graphene device in the channel area. (c) Typical current–voltage curves of a graphene device measured at room temperature for different gate voltages. (d) The corresponding transfer curve measured at the fixed bias voltage $V_{ds}=0.1$ V. The graphene is nearly intrinsic as the Dirac point appears near the zero gate voltage.

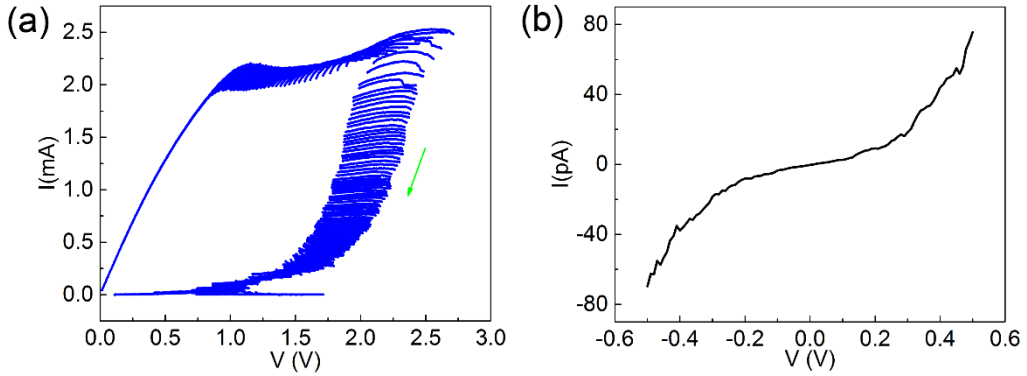


Fig S3 Fabrication of nano-gaps in graphene structures.

(a) Current–voltage traces recorded during the feedback-controlled electro-burning process. (b) Typical current–voltage characteristics of a graphene nano-gap.

3 Electrical characterization of DPP single-molecule FETs

Electrical characterization of other DPP single-molecule FETs with p-type conduction is shown Fig. S4. Different electrical properties originate from the diversity of device configurations. Fig. S5 shows the electrical characterization of Device C with ambipolar conduction. By fitting to the modified single-level model (red dashed line), the HOMO is determined to be $\varepsilon_0 = -0.58$ eV, and the coupling strengths to the source and drain electrodes are $\Gamma_S = 0.52$ meV and $\Gamma_D = 0.5$ meV. From the TVS analysis shown in Fig. S5b the transition voltages at positive and negative polarities are +0.19 V and -0.14 V, respectively.

The electrical characterization of Device E with n-type conduction is shown in Fig. S6. The LUMO is determined to be $\varepsilon_0 = +0.7$ eV, and its coupling strengths to the source and drain electrodes are respectively determined to be $\Gamma_S = 10$ meV and $\Gamma_D = 7.5$ meV. The transition voltages at positive and negative polarities are +0.31V and -0.25 V, respectively.

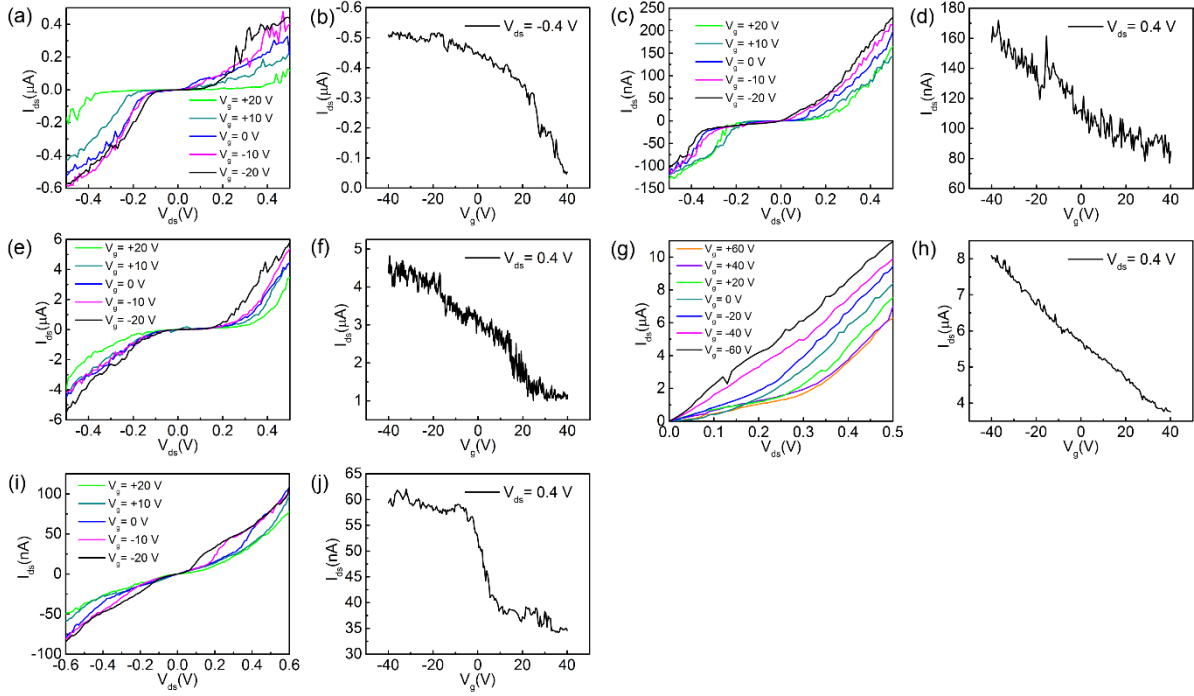


Fig. S4 DPP single-molecule FETs with *p*-type conduction.

(a, c, e, g, i) Current–voltage characteristics measured at 77 K for different gate voltages. (b, d, f, h, j) The corresponding transfer curves measured at the fixed bias voltages of $V_{ds} = -0.4$ V (b) and 0.4 V (d, f, h, j).

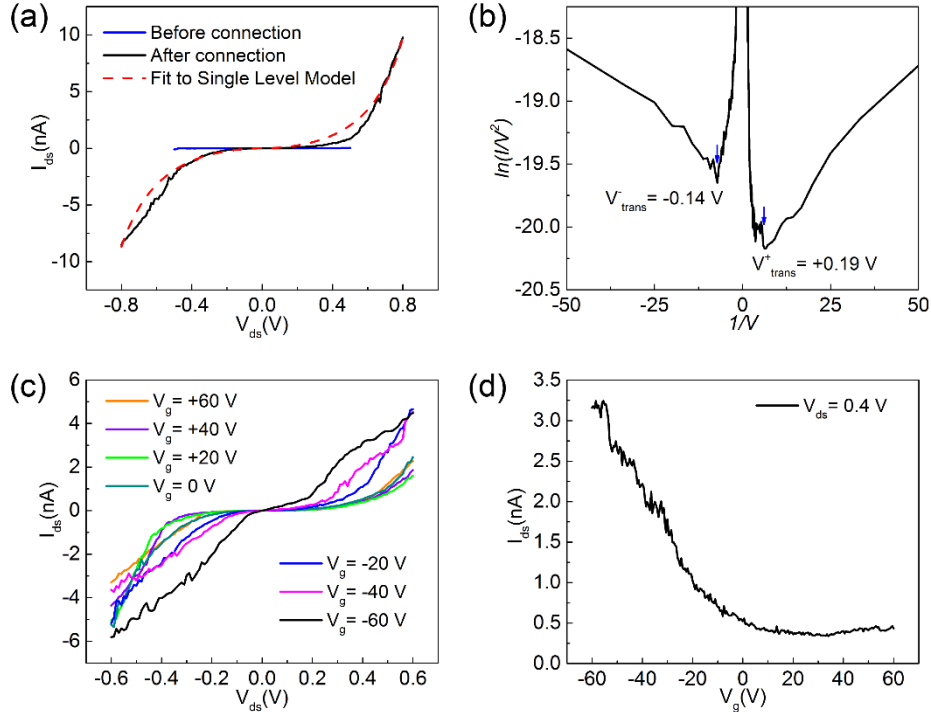


Fig. S5 Electrical characterization of Device C.

(a) Current–voltage characteristics before (blue solid line) and after (black dotted line) phenazine molecule connection at room temperature. The red dashed line is fitted to the modified single-level model. Fitting parameters: the HOMO level $\varepsilon_0 = -0.58$ eV, the coupling strengths to the source and drain electrodes $\Gamma_S = 0.52$ meV and $\Gamma_D = 0.5$ meV.

(b) the F-N plot of the current–voltage curve shown in a. The transition voltages at positive (+0.19 V) and negative (-0.14 V) polarities are labeled by blue arrows.

(c) Current–voltage curves measured at 77 K for different gate voltages. (d) The corresponding transfer curve measured at the fixed bias voltage $V_{ds} = 0.4$ V.

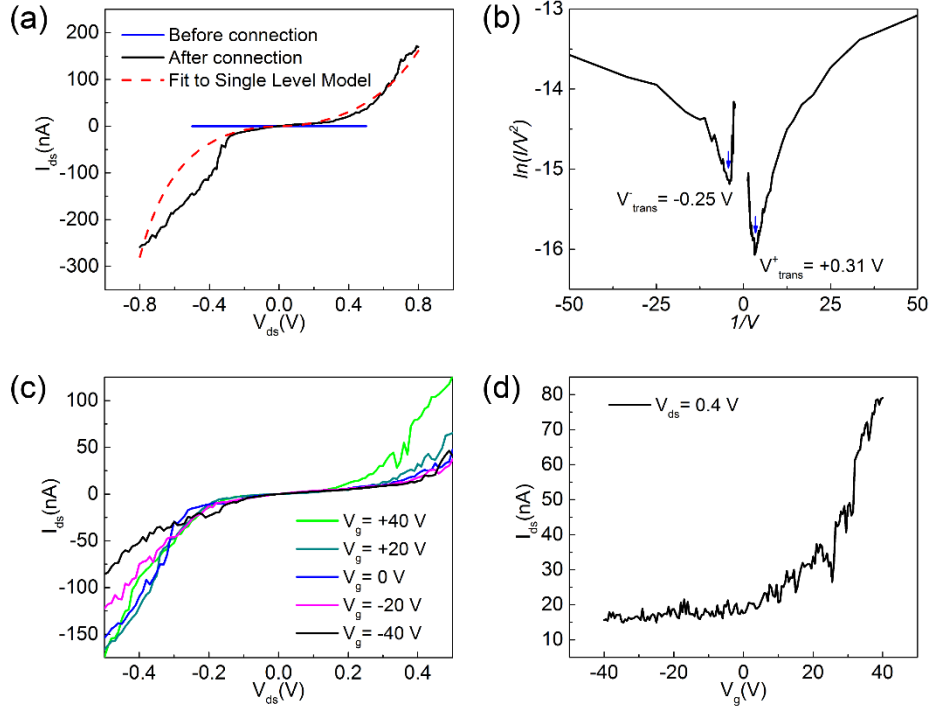


Fig S6 Electric characterization of Device E.

- (a) Current–voltage characteristics before (blue solid line) and after (black dotted line) phenazine molecule connection at room temperature. The red dashed line is fitted to the modified single-level model. Fitting parameters: the LUMO level $\varepsilon_0 = +0.7$ eV, the coupling strengths to the source and drain electrodes $\Gamma_S = 10$ meV and $\Gamma_D = 7.5$ meV.
 (b) the F-N plot of the current–voltage curve shown in a. The transition voltages at positive (+0.31 V) and negative (−0.25 V) polarities are labeled by blue arrows.
 (c) Current–voltage curves measured at 77 K for different gate voltages. (d) The corresponding transfer curve measured at the fixed bias voltage $V_{ds} = 0.4$ V.